Conference Proceedings

Solar World Congress 2015
Daegu, Korea, 08 – 12 November 2015

REDOX AND FLUIDIZATION PERFORMANCES OF Co_3O_4/CoO FOR SOLAR THERMOCHEMICAL ENERGY STORAGE

N. Gokon[1,*], S. Yokota[2], H.S. Cho[1], T. Hatamachi[3], T. Kodama[3]

[1] Center for Transdisciplinary Research, Niigata University, 8050 Ikarashi 2-nocho, Nishi-ku, Niigata 950-2181, Japan

[2] Graduate School of Science and Technology, Niigata University, 8050 Ikarashi 2-nocho, Nishi-ku, Niigata 950-2181, Japan

[3] Department of Chemistry & Chemical Engineering, Faculty of Engineering, Niigata University, 8050 Ikarashi 2-nocho, Nishi-ku, Niigata 950-2181, Japan

Abstract

Thermochemical energy storage using redox pair of Co_3O_4/CoO powders was studied for thermal energy storage (TES) using concentrated solar radiation as the energy source. Reversible chemical reactions (reduction – oxidation redox cycles) of oxides under air atmosphere are used to storage significant thermal energy via the enthalpies of the chemical reactions at high-temperature. A promising concept for solar TES is proposed using fluidized bed with Co_3O_4/CoO redox pair. In the present study, the effects of particles size of Co_3O_4/CoO powders on thermochemical storage performances are investigated in order to explore the potential of the material for fluidized-particle bed reactor. The Co_3O_4 powders with particle sizes of 100-200, 200-300, 300-500 and 500-700 μm were used to test redox performances by thermo-gravimetric analysis. A flowability (fluidization state) of Co_3O_4 powders in a fluidized bed reactor for thermochemical energy storage is also examined in this study. A basic relationship between pressure drop of inlet gas and gas flow rate was experimentally examined using bed materials with different particle sizes by a small-scale quartz reactor at ambient pressure and temperature.

Keywords: *Solar thermochemical storage, redox material, Co_3O_4/CoO, Fluidized bed reactor*

1. Introduction

Concentrated solar radiation has some specific properties such as high density, heterogeneous distribution of thermal flux, and frequent thermal transients due to the fluctuating insolation resulting from cloud passage. Thus, concentrated solar power (CSP) system requires to effectively storage the high temperature heat in order to realize long-term operation of the system such as around-the clock operation. Also, solar chemical reactor for solar hydrogen production can convert the high-temperature solar heat into chemical fuels via endothermic thermochemical process, for example, two-step water-splitting cycle, methane reforming and gasification of carbonous materials.

Thermal energy can be stored as sensible, latent or thermochemical heat. Thermochemical heat storage (TCS) presents higher energy densities than sensible or latent heat, and it can be used at higher temperature ranges. The thermochemical heat storage consists of charge, storage and discharge steps. The high-temperature heat provided by concentrated solar radiation is used to proceed with an endothermic reaction of reversible chemical reaction during the charge step. Thus, the high-temperature heat can be chemically stored as reaction products. Finally, the reaction products are used in order to recover the high-temperature heat through an exothermic reaction of reversible chemical reaction during the discharge step. Redox pair operating at temperature range of 600-1000ºC, much higher than the operational limit of 600ºC for current state-of-the-art molten nitrate salt heat transfer fluid, is eligible for next–generation CSP plants (Agrafiotis et

doi:10.18086/swc.2015.04.25 Available at http://proceedings.ises.org

al., 2014a, Carrillo et al., 2014), while redox pair at temperature range of 800-1000ºC works for solar methane reforming and gasification of carbonous materials to produce hydrogen and synthetic gas.

The choice of the redox pair for TCS are important with regard to thermodynamics, energy storage capacity, material costs, reaction kinetics, toxicity and cyclic behavior (Worner et al., 2012). A redox cycle through a hercynite cycle ($FeAl_2O_4$) was studied for TCS by the University of Colorado (Ehrhart et al., 2014). A redox pair of CuO/Cu_2O was recently tested for TCS (Alonso et al., 2015). Wong evaluated various metal oxides as a TCS medium by thermodynamic calculation and experimental analysis (Wong, 2011). Among those which were suitable for TCS, a redox pair of Co_3O_4/CoO showed beat re-oxidation kinetics. Recently, Co_3O_4/CoO redox pair has been studied for some TCS performances from the viewpoints of thermodynamic analysis, material testing and reactor/heat exchanger developments (Schrader et al., 2015, Neises et al., 2012, Tescari et al, 2014, Carrillo et al., 2014, Pagkoura et al., 2014, Agrafiotis et al., 2014a and Agrafiotis et al., 2015b).

Co_3O_4/CoO redox pair store and release energy through the following redox reaction:

$$Co_3O_4 \rightarrow 3CoO + 1/2O_2 \qquad \Delta H = 196.5 \text{ kJ/mol-reactant at } 950\ ^{\circ}C \qquad (1)$$

Co_3O_4 presents a high potential for TCS and fits the operation temperature for CSP plants (Wong, 2011) and solar chemical reactor. A promising concept for CSP plants provided with a volumetric air central receiver using Co_3O_4/CoO redox pair is proposed and studied (Agrafiotis et al., 2014a).

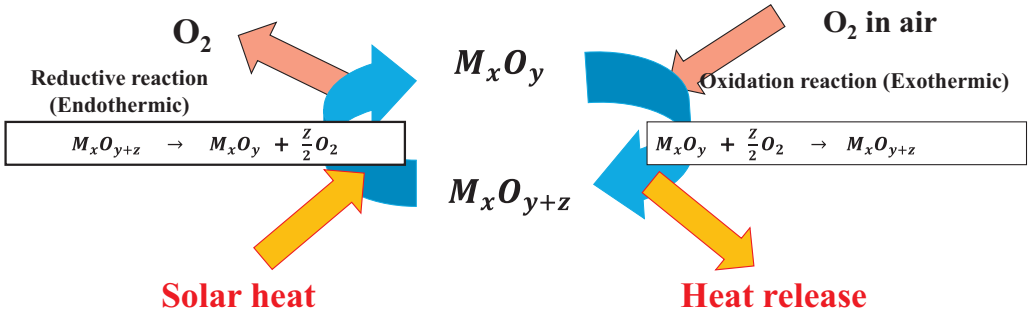

Figure 1. Schematic diagram of thermochemical energy storage by M_xO_{y+z}/M_xO_y redox pair.

The present authors in Niigata University have been developing windowed receivers/reactors prototype using fluidized bed of reacting (coal cokes, and metal oxides) or chemically-inert (quartz sand) particles, and have proposed to combine the windowed solar chemical reactor/receiver with a newly developed solar reflective tower or beam-down optics. In the present study, the effects of particles size of Co_3O_4/CoO powders on TCS performances are investigated in order to explore the potential of the material for fluidized-particle bed reactor. A flowability (fluidization state) of Co_3O_4 powders in a cold testing of fluidized bed reactor is also examined in this study.

2. Experimental procedure

2.1. Preparation of Co_3O_4 powders for fluidization testing and thermochemical storage testing

Co_3O_4 powders were purchased from Japan Pure Chemical Co., Ltd in Japan. The Co_3O_4 powders were divided into four particle size ranges: 30–100 μm, 100–300 μm, 300–500 μm, and 500–700 μm. The Co_3O_4 powders of all particle sizes were prepared for investigation of fluidization state in a cold testing of fluidized bed reactor and thermochemical storage testing by using thermogravimetry reactor (Thermo plus EVO 2/TG-DTA series manufactured by Rigaku Co. ltd.) and a differential scanning calorimeter (DSC). The Co_3O_4 powder of 30–100 μm and 500–700 μm size were used as the redox material for investigation on redox performances.

2.2. Fluidization testing of Co_3O_4 powders by a small-scale quartz reactor of fluidized bed

A basic relationship between pressure loss of inlet gas and outlet gas was experimentally examined using Co_3O_4 powders with different particle sizes by a small-scale quartz reactor at ambient temperature in order to examine a flowability (fluidization state) of Co_3O_4 powders in a fluidized bed reactor for thermochemical storage processes. Fig. 2 shows an experimental setup for flowability test of fluidizing particles by using a small-scale quartz reactor. The diameter of the quartz reactor tube was 25 mm with a thickness of 2 mm, and a length of 48 mm. A porous quartz frit (the hole diameter is 40 μm) was used as the distributor for the small-scale quartz reactor.

Each size of Co_3O_4 powders (21-28 gram) was tested as the fluidized bed of chemical storage material. The Co_3O_4 powder was put into the quartz reactor. The bed height of Co_3O_4 powder inside the reactor is 25 mm for all the particle size. Air was flowed upwards from the bottom of the reactor through the distributor to create the fluidization of Co_3O_4 powder under various air flow rates. A pressure difference for the inlet and outlet gas was measured under various gas flow rates by manometer. The relationship between pressure loss of fluidization gas and flow rate was experimentally examined using each size of Co_3O_4 powder.

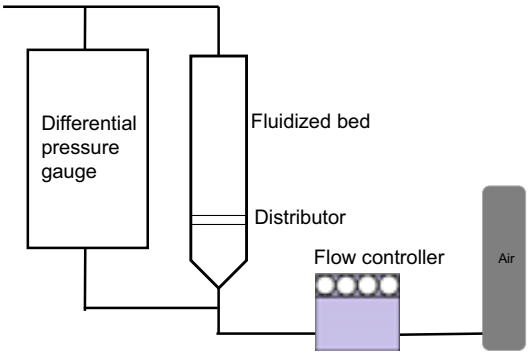

Figure 2. Flowability test of CeO_2 particles ranged in variety size by a small-scale quartz reactor.

2.3. Thermochemical storage testing by thermogravimetry reactor and DSC measurement

Approximately 100 mg of Co_3O_4 powder was packed into a platinum cup (5 mm in diameter and 5 mm deep), and mounted on the balance in a ceramic reaction chamber. Fig. 3 shows experimental set-up for thermogravimetry reactor used for endothermic thermal reduction (TR) step of Co_3O_4 powder and exothermic air oxidation (AO) step of CoO powder. The Co_3O_4 powder mounted in the thermogravimetry reactor were first heated to 1373K with different heating rates of 10 K/min and 30 K/min using an electric furnace, while passing air (purity 99.9%) through the reactor at a flow rate of 0.2 $dm^3 \bullet min^{-1}$(nor) controlled by mass flow controller (KOFLOC RK1700), in order to perform the TR step for heat charging. The temperature of the Co_3O_4 powder was controlled using an R-type thermocouple in contact with the platinum cup. The powder was heated at a constant temperature of 1373 K for 30 min. The weight change of the powder by O_2 release during AO step for heat discharging was measured against time in order to monitor a degree of reaction fraction of AO step.

A reaction conversion α for O_2 release and uptake during the TR and AO step was defined as follows:

$$\alpha = \frac{m - m_i}{m_f - m_i} \quad (2)$$

where m and m_i are weight of sample at time t and initial weight, respectively; m_f is final weight when an ideal reaction proceeds. In thermogravimetry, the reaction fraction α was calculated by the measured weight change of sample.

Subsequently, the powder subjected to the TR step was cooled to 1073 K in air stream at a flow rate of 0.2 $dm^3 \bullet min^{-1}$(nor) to perform the subsequent AO step in an electric furnace of thermogravimetry reactor, and the AO step was continued for 30 min. The temperature of the sample was too controlled using a R-type thermocouple in contact with the platinum cup. The weight change of the powder by O_2 uptake during AO

step was measured against time in order to monitor a degree of reaction fraction of AO step.

The TR and AO steps were alternately repeated three times.

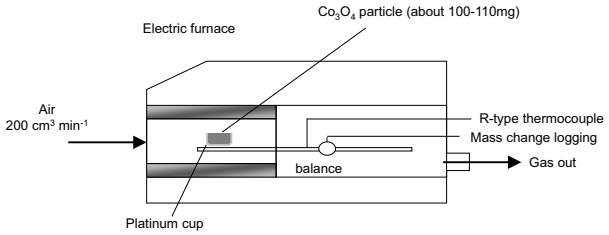

Figure 3. Schematic of the thermogravimetry reactor for thermochemical energy storage using Co_3O_4/CoO redox pair.

The chemical energy storage capacity at the redox temperature and sensible heat capacity arising from the Co_3O_4 and CoO powders were measured for the Co_3O_4/CoO redox pair using a differential scanning calorimeter (DSC). Also, the redox temperature of Co_3O_4/CoO redox pair was estimated from a measurement of endothermic and exothermic peaks by DSC. The specific heat C_p values of the Co_3O_4/CoO redox pair before and after the cyclic reaction were also measured to estimate the dependence of the sensible heat on the temperature using the DSC. The programmed heating and cooling rates for the DSC measurements were as follows: 1) a heating rate of 10 K/min between room temperature and 1000 °C, 2) 30 min at 1000 °C, 3) a cooling rate of 10 K /min down to 800 °C, and 4) 30 min at 800 °C. The heating/cooling cycle in the DSC was repeated three times in air stream.

3. Results and Discussion

3.1. Fluidization testing of Co_3O_4 powders by a small-scale quartz reactor of fluidized bed

Fig. 4 shows results for fluidization testing using a fluidized bed reactor. The Co_3O_4 powder with different particle sizes between 50 and 700 μm diameter was used and tested as a bed material for the fluidized bed reactor. For the particle size of 50-100 μm, a pressure loss initially increased with superficial gas velocity of inlet gas, and reached the small peak of 690 Pa at a velocity of 0.068 m·sec^{-1}. Subsequently, the pressure loss plateaued and then increased to about 1460 Pa. This behavior of pressure loss for the superficial gas velocity indicates that the velocity of 0.068 m·sec^{-1} corresponds to start a fluidization of Co_3O_4 powder; a minimum superficial gas velocity (U_{mf}) = 0.068 m·sec^{-1} for the particle size 50-100μm. Similarly, for the particle size of 100-300 μm, a peak value for pressure loss was reduced to about 510 Pa in comparison to that for the particle size 50-100 μm, while the value of U_{mf} slightly decreased to 0.054 m·sec^{-1}. In addition, the plateau region where the value for pressure loss is stable for increasing superficial gas velocity of inlet gas, was apparently expanded when the particle size was used.

According to the results in this figure, the fluidization state can be categorized into three regions: fixed layer, bubble fluidization and turbulent fluidization regions. Firstly, a pressure loss increases with increasing a superficial gas velocity. This region was called to fix bed layer, and U_{mf} was corresponded to the following value for the peak of the pressure loss. It was observed that hereafter, a particle started fluidizing. By further increasing a superficial gas velocity, the pressure loss plateaued. In this region, a particle bed made a bubbling fluidization. Beyond the bubbling fluidization, the pressure loss increased again, a particle bed formed a turbulent fluidization. The fluidization state aimed in this study is a lower superficial gas velocity and a mild fluidization of a particle bed in the reactor. Thus, a bubble fluidization was targeted in this study. Based on the experiments of fluidization testing of Co_3O_4 powder, the powder with a smaller size which enables it to make a bubbling fluidization under a lower passing air are favorable for the fluidized bed reactor operating a thermochemical energy storage.

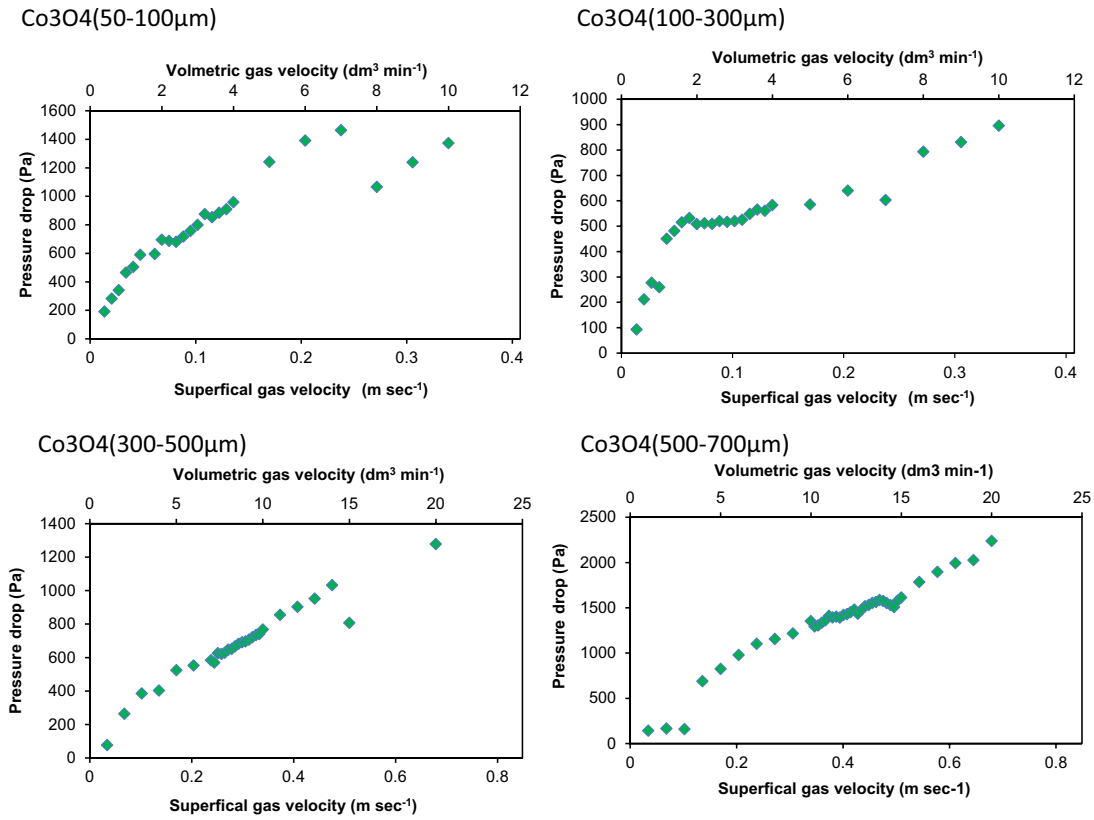

Figure 4. Pressure drop of fluidized bed using various Co_3O_4 powder size

3.2. Thermochemical storage testing by thermogravimetry and DSC measurements

Fig. 5 shows redox reactivity and cyclic performances of Co_3O_4 powder with different particle sizes by thermogravimetry analysis. The heating–cooling operation was performed by a trapezoid mode in order to drive each step as much as possible at temperature of 1100°C and 800°C. For the particle size of 30-100 μm, the weight of sample rapidly decreased with increasing temperature of the sample and reached almost stoichiometric weight change of the sample (Co_3O_4 = 3CoO + 1/2O_2) during TR step. The conversion α of HC step was 99.7, 99.4 and 99.5% for 1st, 2nd and 3rd cycles, respectively. Subsequently, when temperature of the sample decreased in the AO step, the sample returned back to almost initial weight (3CoO + 1/2O_2 = Co_3O_4). The conversion α of AO step was 99.1, 99.2 and 98.6% for 1st, 2nd and 3rd cycles, respectively. Similarly, the weight change of sample for the particle size of 500-700 μm presented superior reactivity and cyclic stability as well as that for particle size of 30-100 μm. Thus, the redox reactivity and cyclic reactivity was independent of the particle size of Co_3O_4 powder.

Fig. 6 shows reaction rate of the Co_3O_4/CoO redox during TR and AO steps for Co_3O_4 powder with the particle size of (a) 30-100 μm and (b) 500-700 μm. The heating–cooling operation was performed by a trapezoid mode. The reaction rate in each step was expressed by a time-derivative of reaction conversion $\frac{d\alpha}{dt}$ for O_2 release and uptake during the TR and AO step. For the particle size of 30-100 μm, the temperature that TR step starts was about 910°C at all cycles. The peak rate in the TR step was $\frac{d\alpha}{dt}$ = about 0.3 at temperature of 945°C. The profiles of reaction rate were reproducibly observed in the TR step at all cycles. On the other hand, for the particle size of 500-700 μm, the temperature that TR step starts was about 920°C at all cycles. The peak rate in the TR step was almost the same ($\frac{d\alpha}{dt}$ = about 0.3) at temperature of 945°C. This means that TR step can start with lower (10°C) temperature as a particle size of Co_3O_4 powder is smaller, but the peak rate in TR step is independent of the particle size. In the case of AO step, the

temperature that AO step starts was almost the same (800°C) with the particle size of 30-100 μm and 500-700 μm, thus was independent of particle size. The reaction rate at a maximum in AO step was 840-850°C, and lower than that for TR step. The results indicate that oxidation reaction of CoO is rate-determining step for thermochemical storage using Co_3O_4/CoO redox pair.

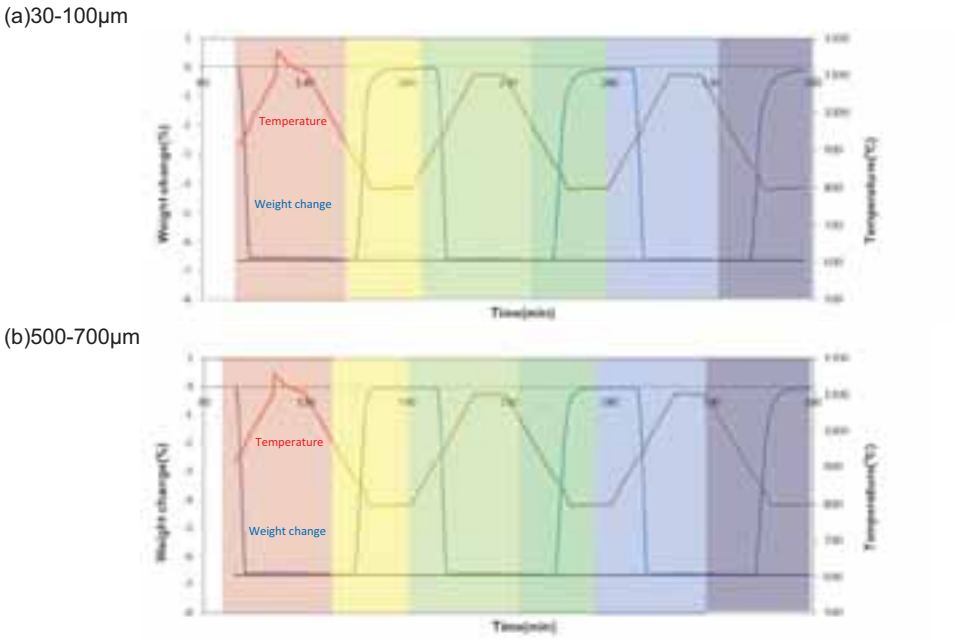

Figure 5. Redox reactivity and cyclic reactivity of Co_3O_4 powder with the particle sizes of (a) 30-100 μm and (b) 500-700 μm. Red and blue lines are temperature and weight change of the sample, respectively. The heating–cooling operation was performed by a trapezoid mode.

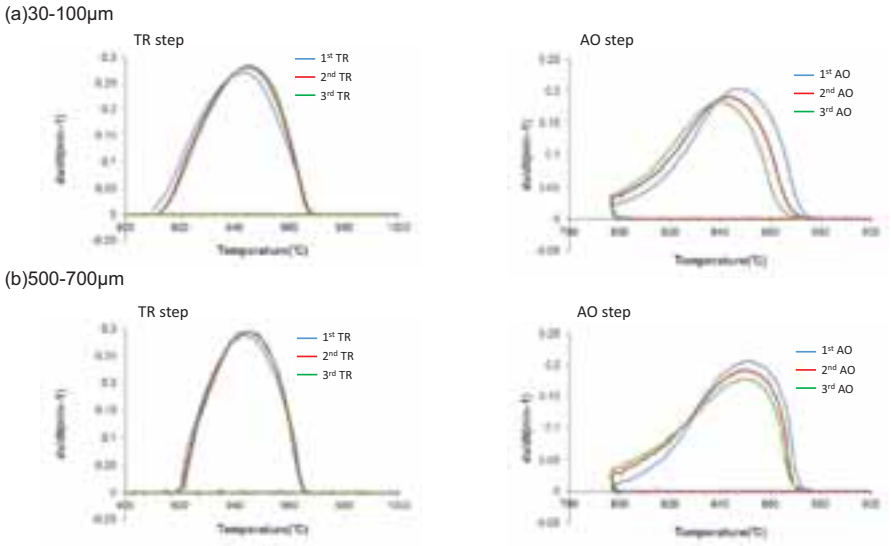

Figure 6. Reaction rate of the Co_3O_4/CoO redox during TR and AO steps for Co_3O_4 powder with the particle size of (a) 30-100 and (b) 500-700 μm. The heating–cooling operation was performed by a trapezoid mode.

Fig. 7 shows comparison for weight change of powder sample with the particle sizes of 30-100 μm and 500-700 μm during TR and AO steps. In the experiments, the samples were subjected to each step without keeping constant temperature of 1100°C for TR step and 800°C for AO step. Namely, the heating–cooling operation was performed by a rectangle mode in order to simulate a heat charging/discharging of Co_3O_4/CoO redox by using a fluidized bed reactor under a concentrated solar radiation. The thermal reduction of Co_3O_4 into CoO proceeded completely for both particle sizes. However, the air oxidation of CoO into Co_3O_4 was

apparently slower for the particle size of 30-100 μm than for that of 500-700 μm in the temperature range of 700-850°C. In order to compare the oxidation rate of CoO during AO step under the heating (charging)-cooling (discharging) operation, the reaction rate of the Co_3O_4/CoO redox during TR and AO steps was plotted against reaction temperature. The plot of reaction rate is shown in Fig. 8. The profiles of reaction rate were reproducibly observed in the TR and AO steps at all cycles. As seen in Fig. 8(a), the temperatures that TR step starts were 915°C for the particle size of 30-100 μm and 920°C for 500-700 μm. Also, the temperatures that TR step terminates were about 965°C for both particle sizes. Further, a peak rate in the TR step was $\frac{d\alpha}{dt}$ = about 0.3 at temperature of 945°C. The temperatures and peak rate for the TR step were almost the same with the results by the different operation mode. However, as seen in Fig. 8(b), for the AO step, the temperatures that AO step starts were 890°C for the particle size of 30-100 μm and 880 °C for 500-700 μm. Also, the temperatures that AO step terminates were 780°C for the particle size of 30-100 μm and 790°C for 500-700 μm. The results for reaction temperatures mean that a temperature region for the AO step expands further high- and low-temperature as a particle size of Co_3O_4 is smaller. The peak rare in the AO step was greater for the particle size of 500-700 μm than that for 30-100 μm. The peak rate in the AO step was $\frac{d\alpha}{dt}$ = about 0.20 at temperature of 865°C for the particle size of 30-100 μm, while that was $\frac{d\alpha}{dt}$ = about 0.22 at temperature of 855°C for 500-700 μm. The temperatures and peak rate for the AO step were different by the operation modes.

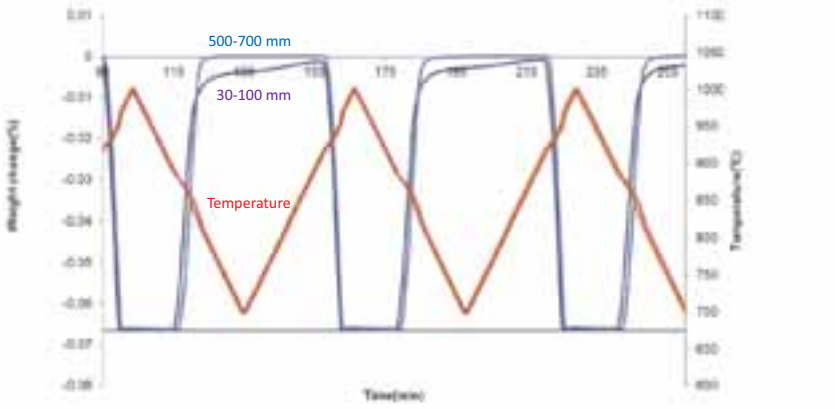

Figure 7. Redox reactivity and cyclic reactivity of Co_3O_4 powder with the particle sizes of 30-100 and 500-700 μm. Red and blue lines are temperature variation and weight change of the sample, respectively. The heating–cooling operation was performed by a rectangle mode.

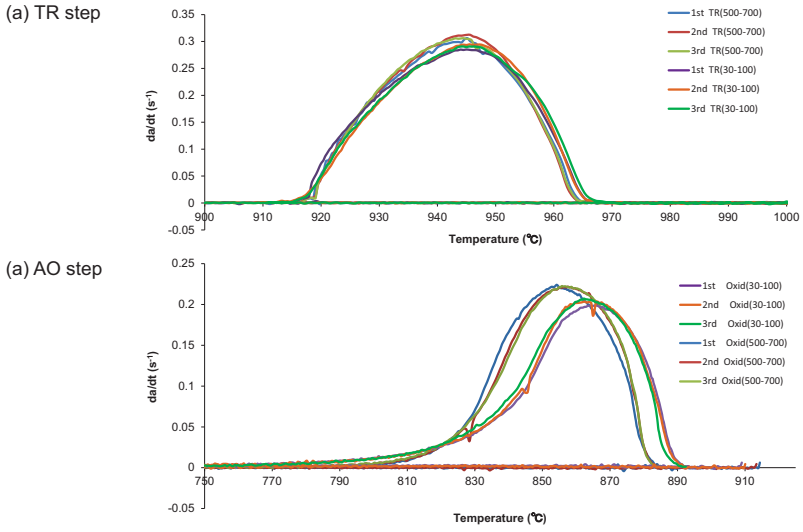

Figure 8. Reaction rate of the Co_3O_4/CoO redox during TR and AO steps for Co_3O_4 powder with the particle size of 30-100 and 500-700 μm at (a) TR and (b) AO steps. The heating–cooling operation was performed by rectangle mode.

Fig. 9 shows the DSC results for the thermal storage capacities of the Co_3O_4/CoO redox material with particle size of (a) 30-100 and (b) 500-700 μm in the charging and discharging modes. The amounts of thermochemical heat storage during the charging and discharging modes were measured at the peak area. For the results of the 30-100μm, as seen in Fig. 9(a), there was a major endothermic peak at temperatures of 949–951°C during the TR step, while a major exothermic peak was observed at temperatures of 853–866°C during the AO step in the 3 cycles. The endothermic and exothermic peak corresponded to the Co_3O_4/CoO redox reaction. The enthalpy changes, ΔH, ($Co_3O_4 = 3CoO + 1/2O_2$ for an endothermic TR step; $3CoO + 1/2O_2 = Co_3O_4$ for an exothermic AO step) were estimated from an integration of the peak area. In addition, the reaction conversions, α, for each step were calculated from the theoretical enthalpy changes, $\Delta H_{theoretical}$. The values of $\Delta H_{theoretical}$ were calculated by thermodynamic software of Factsage. The values of ΔH and α were listed in Table 1. The values of ΔH and α for the 1st TR step were slightly less than those for the 2nd and 3rd TR steps, but each step could almost stoichiometrically charge and discharge. Thus, the values of ΔH and α indicate that the Co_3O_4/CoO redox reaction ideally proceeded in viewpoint of quantitative thermal charging/discharging. For the results of the 500-700 μm, as seen in Fig. 9(b), there was a major endothermic peak at temperatures of 950–954°C during the TR step, while a major exothermic peak was observed at temperatures of 854–862°C during the AO step in the 3 cycles. The endothermic and exothermic peak corresponded to the Co_3O_4/CoO redox reaction was observed at almost same temperature, respectively. The values of ΔH and α for the particle size were listed in Table 2. The results for ΔH and α indicate that the particle size did not impact on the values of ΔH and α in quantitative viewpoint (Fig. 5 and 7), but effect on a kinetic viewpoint (Fig. 6 and Fig 8(b)).

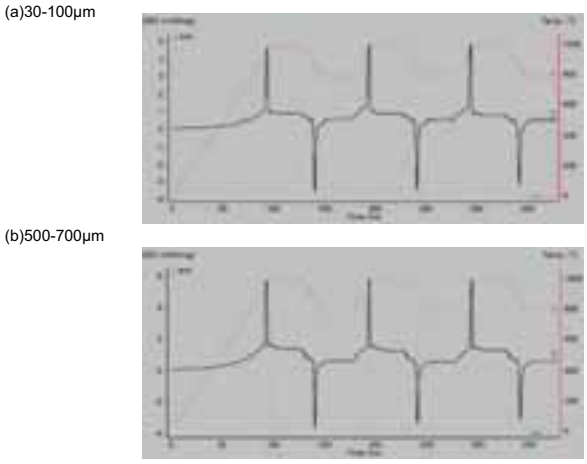

Figure 9. DSC analysis of Co_3O_4/CoO redox material with particle size of (a) 30-100 and (b) 500-700 μm. The heating–cooling operation was performed by a trapezoid mode.

In addition to the thermochemical heat storage based on the value of ΔH, the specific heat values C_p, depending on the temperature in the range of 800–1000°C, were experimentally measured for the Co_3O_4/CoO redox material, and the sensible heat was experimentally estimated to evaluate the thermal storage performances. As a reference, the values of the heat storage capacities for a molten carbonate salt (Na_2CO_3) were calculated using the thermodynamic equilibrium software FactSage ver 6.4. Fig. 10 shows the heat storage capacities per unit weight for the redox pair with the particle size of 30-100 and 500-700 μm. The values for the heat storage capacities were plotted as a standard based on a temperature of 800°C. As shown in Fig. 10, the discontinuous increments are equivalent to the amounts of thermochemical heat due to the Co_3O_4/CoO redox reaction at reaction temperatures of 930-975°C. A sensible heat from the oxidized solid phase of Co_3O_4 enhanced the heat storage capacities in the temperatures of 800-930°C. Beyond the reaction temperature over 975°C, sensible heat from the reduced solid phase of CoO contributed to the increase in the heat storage capacity. The heat storage capacity for the redox pair with the particle size of 30-100 μm was almost the same storage level in comparison to that with the particle size of 500-700 μm. Also, the heat storage capacities for the Na_2CO_3 molten salt discontinuously increase due to latent heat of solid-

liquid phase transition at a temperature of 858°C, and has a heat storage capacity of > 500 kg/kJ at temperatures in the range of 858-930°C, which is higher than that for the redox pair. However, the thermochemical heat strongly contributes to enhancing the thermal storage capacities of the redox pair. The thermal storage capacity for the redox pair is two times higher than that of the molten salt at 1000°C. These results indicate that the thermochemical heat storage for the redox pair is available to use in solar thermochemical processes and CSP, as well as that of the carbonate molten salts. From the viewpoint of the temperature range, using the redox pair for thermal storage may be appropriate for the solar tower/beam down receiver system using fluidized particle bed using high-temperature air as a heat transfer fluid.

Table 1 Enthalpy change and reaction conversion in each step for Co_3O_4/CoO redox material with the particles size of 30-100µm.

	1st TR	1st AO	2nd TR	2nd AO	3rd TR	3rd AO
Enthalpy change, Δ*H*	756.1 J/g	-830.5 J/g	812.2 J/g	-829.2 J/g	814.3 J/g	-829.2 J/g
Reaction conversion, α	92.7 %	99.2 %	99.9 %	99.7 %	99.8 %	99.7 %

Table 2 Enthalpy change and reaction conversion in each step for Co_3O_4/CoO redox material with the particles size of 500-700µm.

	1st TR	1st AO	2nd TR	2nd AO	3rd TR	3rd AO
Enthalpy change, Δ*H*	755.6 J/g	-824.4 J/g	812.0 J/g	-822.1 J/g	811.8 J/g	-805.8 J/g
Reaction conversion, α	92.6 %	99.2 %	99.5 %	98.9 %	99.5 %	96.9 %

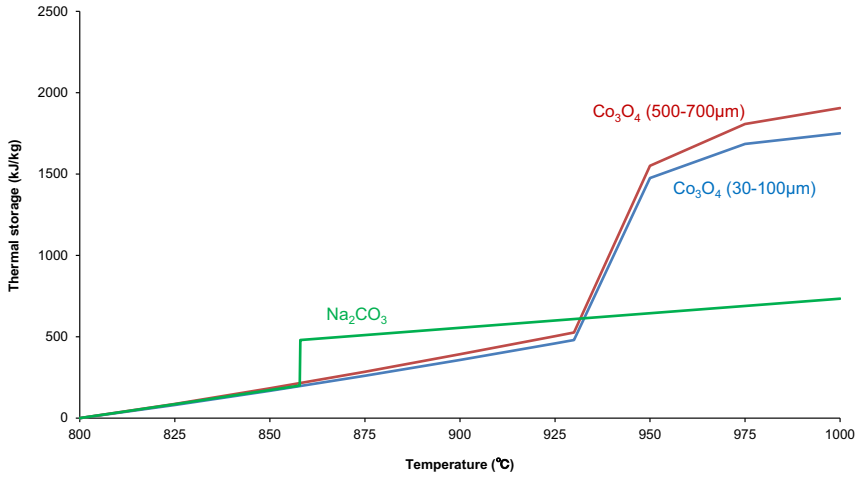

Figure 10. Heat storage capacities per unit weight (kg) for Co_3O_4/CoO redox material. The heat storage capacity at temperature of 800 ºC as a standard is set to zero.

4. Summary

The present authors in Niigata University have been developing windowed receivers/reactors prototype using fluidized bed of reacting (coal cokes, and metal oxides) or chemically-inert (quartz sand) particles, and have proposed to combine the windowed solar chemical reactor/receiver with a newly developed solar reflective tower or beam-down optics. In the present study, the effects of particles size of Co_3O_4/CoO powders on TCS performances were investigated in order to explore the potential of the material for fluidized-particle bed reactor. A flowability (fluidization state) of Co_3O_4 powders in a cold testing of fluidized bed reactor was also examined in this study.

For the fluidization testing of Co_3O_4 powders by a small-scale quartz reactor of fluidized bed, the fluidization state aimed in this study was a lower superficial gas velocity and a mild fluidization of a particle bed in the

reactor. Thus, a bubble fluidization was targeted in this study. Based on the experiments of fluidization testing of Co_3O_4 powder, the powder with a smaller size which enabled it to make a bubbling fluidization under a lower passing air were favorable for the fluidized bed reactor operating a thermochemical energy storage. From the viewpoint of stability of fluidization, the particle size of 100-300 μm showed the minimum pressure loss at the value of U_{mf} among the all particle size tested.

For the thermochemical storage testing by thermogravimetry and DSC measurements, the heating–cooling operation was performed at 1100-800°C by a trapezoid and rectangle modes in order to evaluate a heat charging/discharging performances of Co_3O_4/CoO redox with different particle size. TR step could start with lower (10°C) temperature as a particle size of Co_3O_4 powder was smaller, but the peak rate in TR step was independent of the particle size. Oxidation reaction of CoO was rate-determining step for thermochemical storage using Co_3O_4/CoO redox pair. In DSC measurement, the endothermic and exothermic peak corresponded to the Co_3O_4/CoO redox reaction was observed at almost same temperature, respectively. The results for ΔH and α indicate that the particle size did not impact on the values of ΔH and α in quantitative viewpoint (Fig. 5 and 7), but effect on a kinetic viewpoint (Fig. 6 and Fig 8(b)).

5. References

Agrafiotis, C., Roeb, M., Schmu¨cker, M., Sattler, C., 2014. Exploitation of thermochemical cycles based on solid oxide redox systems for thermochemical storage of solar heat. Part 1: Testing of cobalt oxide-based powders. Solar Energy 102, 189-211.

Agrafiotis, C., Roeb, M., Schmu¨cker, M., Sattler, C., 2015. Exploitation of thermochemical cycles based on solid oxide redox systems for thermochemical storage of solar heat. Part 2: Redox oxide-coated porous ceramic structures as integrated thermochemical reactors/heat exchangers. Solar Energy 114, 440-458.

Alonso, E., Pe´rez-Ra´bago, C., Licurgo, J., Fuentealba, E., Estrada, C. A., 2015. First experimental studies of solar redox reactions of copper oxides for thermochemical energy storage. Solar Energy 115, 297-305.

Carrillo, A. J., Moya, J., Bayón, A., Jana, P., O'Shea, V. A. P., Romero, M., Gonzalez-Aguilar, J., Serrano, D. P., Pizarro, P., Coronado, J. M., 2014. Thermochemical energy storage at high temperature via redox cycles of Mn and Co oxides: Pure oxides versus mixed ones. Solar Energy Materials & Solar Cells 123, 47-57.

Ehrhart, B., Coker, E., Siegel, N., Weimer, A., 2014. Thermochemical cycle of a mixed metal oxide for augmentation of thermal energy storage in solid particles. Energy Procedia 49, 762-771.

Neises, M., Tescari, S., de Oliveira, L., Roeb, M., Sattler, C., Wong, B., 2012. Solar-heated rotary kiln for thermochemical energy storage. Solar Energy 86, 3040–3048.

Pagkoura, C., Karagiannakis, G., Zygogianni, A., Lorentzou, S., Kostoglou, M., Konstandopoulos, A. G., Rattenburry, M., Woodhead, J. W., 2014. Cobalt oxide based structured bodies as redox thermochemical heat storage medium for future CSP plants. Solar Energy 108, 146-163.

Schrader, A. J., Muroyama, A. P., Loutzenhiser, P. G., 2015. Solar electricity via an Air Brayton cycle with an integrated two-step thermochemical cycle for heat storage based on Co_3O_4/CoO redox reactions: Thermodynamic analysis. Solar Energy 118, 485-495.

Tescari, S., Agrafiotis, C., Breuer, S., de Oliveira, L., Neises-von Puttkamer, M., Roeb, M., Sattler, C., 2014. Thermochemical solar energy storage via redox oxides: materials and reactor/heat exchanger concepts. Energy Procedia 49, 1034-1043.

Wörner, A., Binyami, S., Giger, F., Soupart, J.-B., Gonzalez-Aguilar, J., Steinfeld, A., Trettin, R., 2012. The TCS Power Project Thermochemical Energy Storage for Concentrated Solar Power Plants, SolarPACES, Marrakech, Morocco, 2012.

Wong, B., 2011. Thermochemical Heat Storage for Concentrated Solar Power, Final Report for the US Department of Energy, San Diego, CA, USA.